Oddziaływanie proton-neutron w jądrze atomowym

Zygmunt Patyk

Zakład Fizyki Teoretycznej IPJ

Warszawa, 07.10.2009

Streszczenie wykładu

1. **Pomiar mas jader atomowych metodą SMS.**
2. **Własności jąder atomowych dla których zmierzono masy.**
3. **Wielkość przerwy energetycznej w widmie jednocząstkowym otrzymywana z relacji mas.**
4. **Oddziaływanie proton-neutron otrzymane z relacji mas**
5. **Ograniczenia występujące przy interpretacjach powyższych relacji mas.**
6. **Perspektywy pomiarów mas i czasów życia na rozpady alpha, beta i wychwyt elektronu w w FAIR-Darmstadt /ILIMA/.**

Nuclear mass measurement methods at GSI

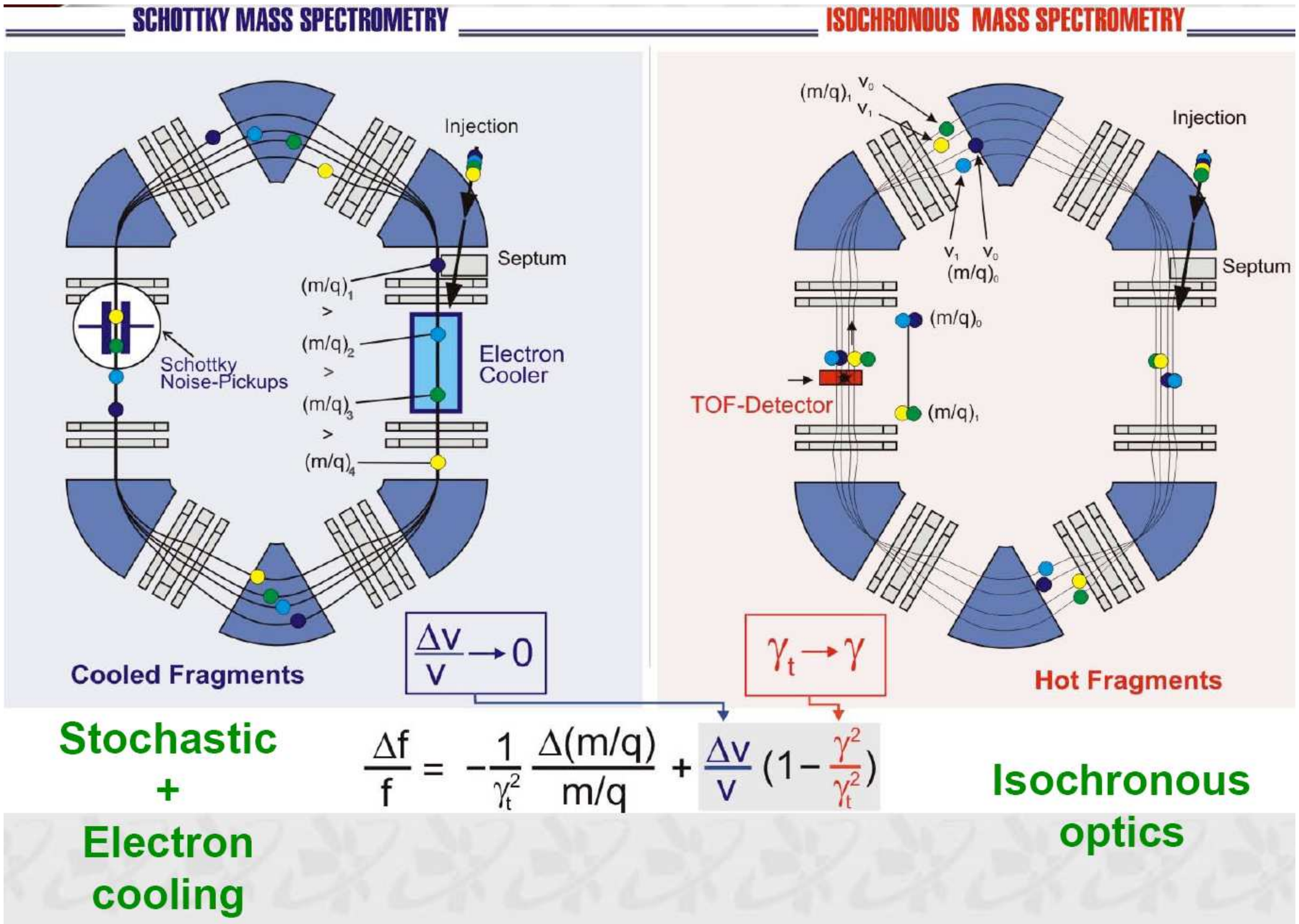

Basic properties

projectile: ^{238}U 670 MeV/u

target in front of FRS: ^{9}Be

Electron cooling: $\delta v/v=10^{-7}$

Masses for near 35 nuclei were measured

Mass measurements

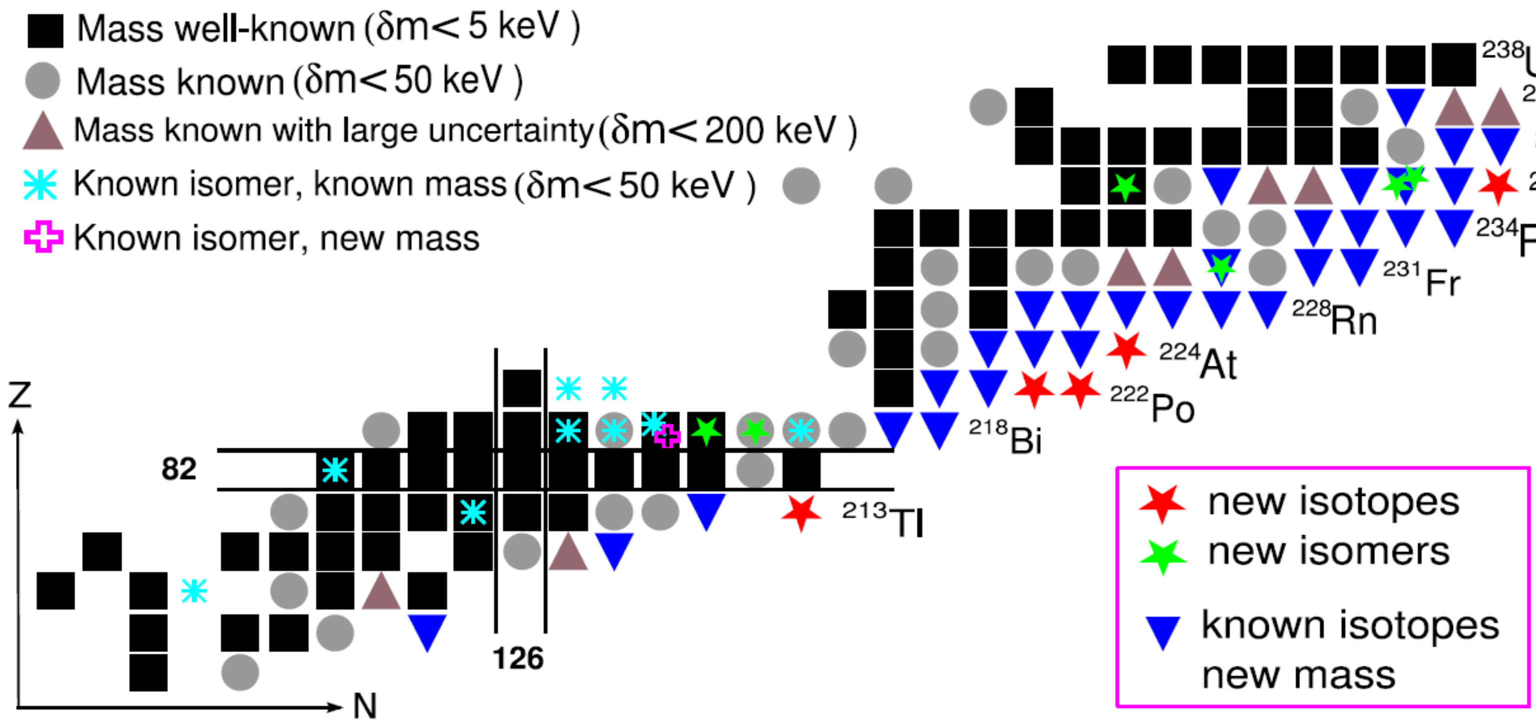

Figure 4.1: Nuclides measured in this experiment in the element range of Ir – U. The information for known masses are taken from the compilation AME2003.

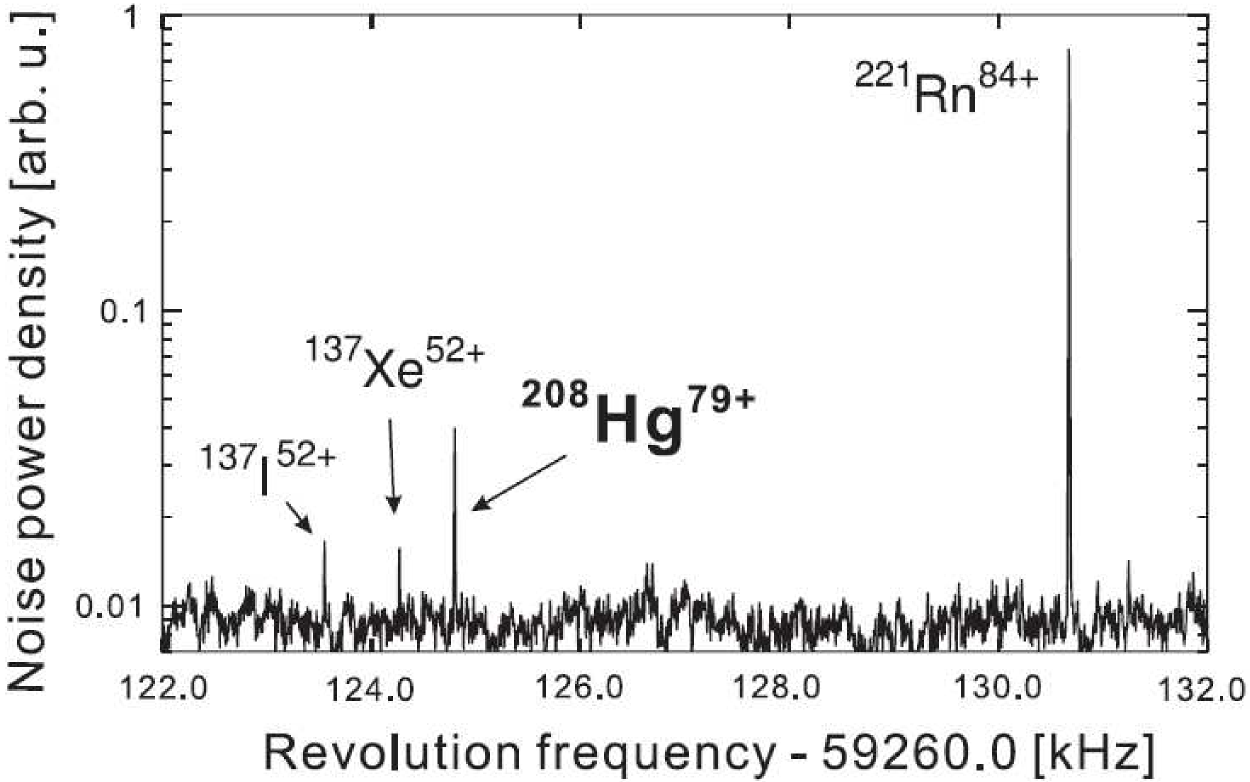

FIG. 1. A 10 kHz part of the measured revolution frequency spectrum. For this spectrum the electron cooler voltage and current were set to $U_c = 198$ kV and $I_c = 400$ mA, respectively. A peak of hydrogenlike $^{208}Hg^{79+}$ ions is at about 125 kHz. The masses of $^{137}I^{52+}$, $^{137}Xe^{52+}$ and $^{221}Rn^{84+}$ ions are experimentally known [30] and can be used for the calibration.

RAPID COMMUNICATIONS

PHYSICAL REVIEW C VOLUME 49, NUMBER 2 FEBRUARY 1994

Observation of the new neutron-rich nuclide ^{208}Hg

Zhang Li, Jin Genming, Zhao Jinhua, Yang Weifan, Yang Yongfeng, Zhao Zhizheng, Zheng Jiwen, Sun Xiurong, Wang Jicheng, Li Zongwei, Qin Zhi, Guo Guanghui, Luo Yixiao, Jan Zylicz,* and Jing-ye Zhang†

Institute of Modern Physics, Academia Sinica, Lanzhou 730000, China

(Received 1 July 1993)

The new neutron-rich isotope ^{208}Hg was observed for the first time in the reaction products from a thick $^{\mathrm{nat}}$Pb target bombarded by a 30 MeV/nucleon ^{12}C beam. A high efficiency release, separation, and collection of Hg products were of success with a good selectivity by using a special off-line gas-phase thermochromatographic process followed by a liquid-liquid procedure which was developed in the present work. The assignment of ^{208}Hg was based on the identification of its β^- decay daughter ^{208}Tl observed in the periodically extracted Tl element sample growing in the separated Hg element product solution. In the γ spectra of the Tl samples a 2614.6-keV γ activity with a half-life 191^{+104}_{-50} s was observed, which could only be assigned to the daughter ^{208}Tl of ^{208}Hg β^- decay. The measured ^{208}Hg half-life was 42^{+23}_{-12} min and the average production cross section for the energy of the ^{12}C beam ranging from 30 MeV/nucleon to 5 MeV/nucleon and the effective target thickness of 670 mg/cm^2 was deduced to be $1.1^{+1.0}_{-0.5}$ μb. Moreover, in the time-successive γ spectra of the separated Hg sample, a 473.5-keV γ activity corresponding to the γ transition of 4^+ to ground state (5^+) of ^{208}Tl was observed and found to have the same half-life as the ^{208}Hg β^- decay within the error range of the present work. A theoretical discussion for the obtained half-life of ^{208}Hg is given.

PACS number(s): 21.10.Tg, 23.40.Hc, 27.80.+w

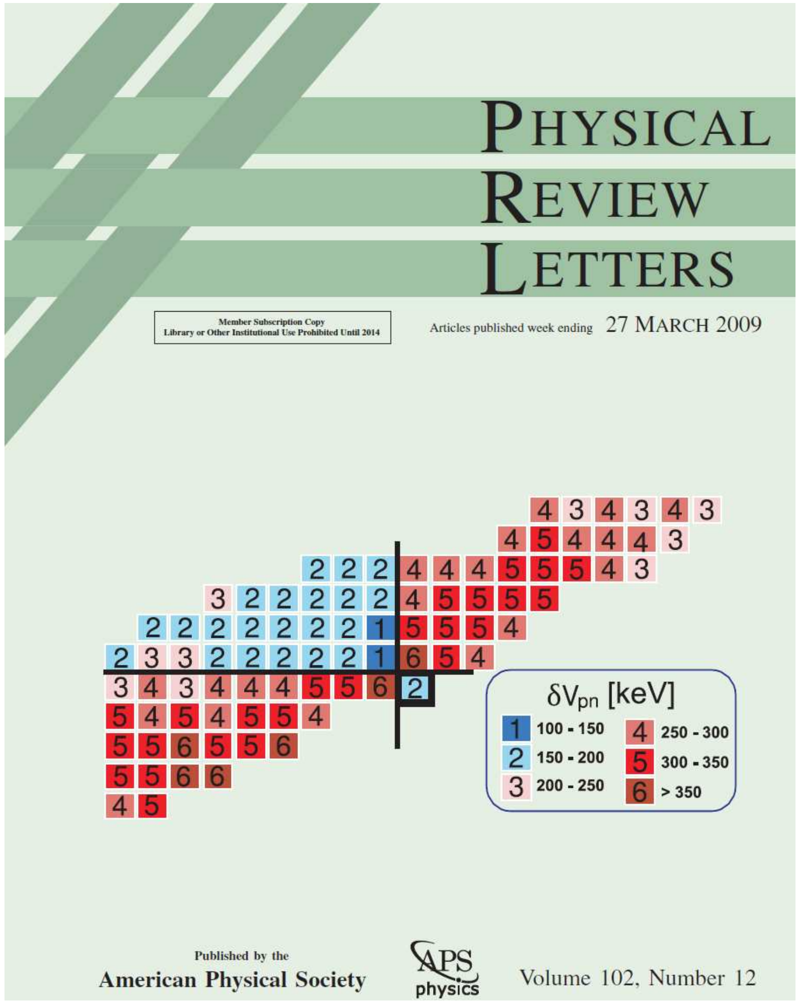

Schottky Mass Measurement of the ^{208}Hg Isotope: Implication for the Proton-Neutron Interaction Strength around Doubly Magic ^{208}Pb

L. Chen,[1,2] Yu. A. Litvinov,[1,*] W. R. Plaß,[1,2] K. Beckert,[1] P. Beller,[1] F. Bosch,[1] D. Boutin,[2] L. Caceres,[1] R. B. Cakirli,[3,4] J. J. Carroll,[5] R. F. Casten,[4,6] R. S. Chakrawarthy,[7] D. M. Cullen,[8] I. J. Cullen,[9] B. Franzke,[1] H. Geissel,[1,2] J. Gerl,[1] M. Górska,[1] G. A. Jones,[9] A. Kishada,[8] R. Knöbel,[1] C. Kozhuharov,[1] S. A. Litvinov,[1] Z. Liu,[9] S. Mandal,[1] F. Montes,[10] G. Münzenberg,[1] F. Nolden,[1] T. Ohtsubo,[11] Z. Patyk,[12] Zs. Podolyák,[9] R. Propri,[5] S. Rigby,[8] N. Saito,[1] T. Saito,[1] C. Scheidenberger,[1,2] M. Shindo,[13] M. Steck,[1] P. Ugorowski,[5] P. M. Walker,[9] S. Williams,[9] H. Weick,[1] M. Winkler,[1] H.-J. Wollersheim,[1] and T. Yamaguchi[14]

„Experimental” gap for Pb isotopes

2p
\+ 2p – 2p 2p
Z-2 Z-2 Z-2 Z-2

$$2G_p = (M(Z-2,N) + M(Z+2,N) - 2M(Z,N))c^2$$

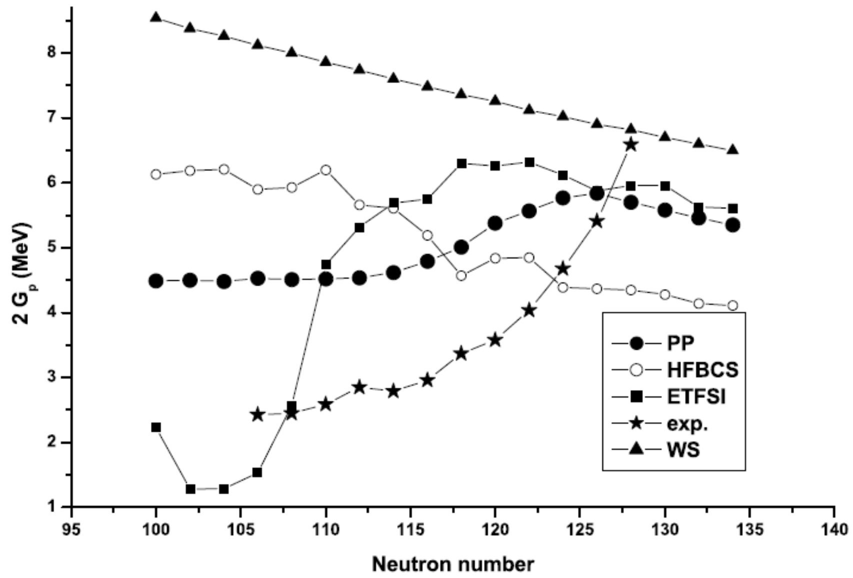

Fig. 5. The double proton gap (in MeV) calculated according to Eq. (1) in the macroscopic–microscopic (full circles), ETFSI (full squares) and HFBCS (open circles) approaches plotted as a function of neutron number. The experimental proton gap is indicated by stars. Also the gap in the proton single particle spectrum of the Woods–Saxon (WS) potential around the Fermi level (triangles) is presented.

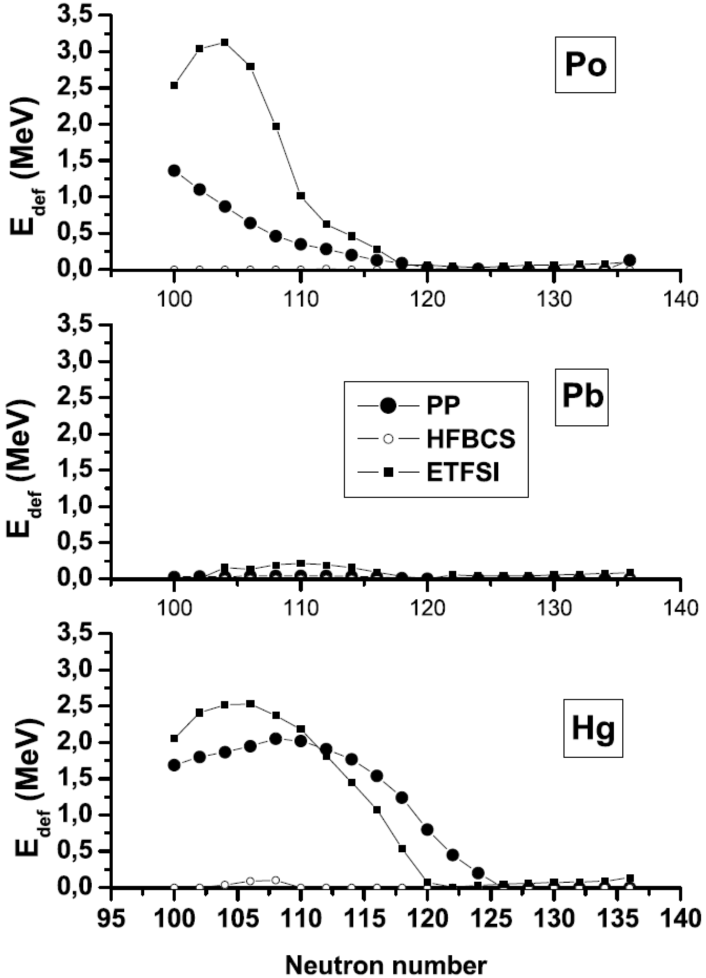

Fig. 2. Deformation energy (in MeV) for macroscopic–microscopic (full circle), ETFSI (full square) and HFBCS (open circle) models plotted as a function of neutron number. Hg, Pb and Po isotopes are studied.

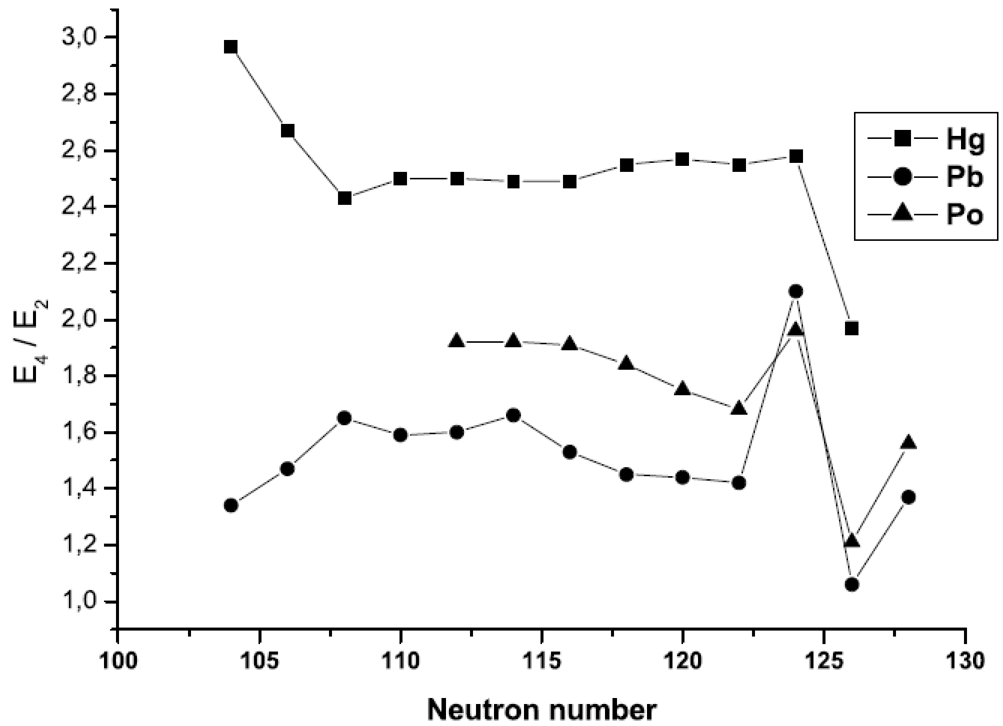

Fig. 3. The experimental ratio [10] E_4 to E_2 for Hg (square), Pb (circle) and Po (triangles) isotopes illustrated as a function of neutron number.

Uśrednione „doświadczalne” oddziaływanie walencyjnych protonów i neutronów

$$\delta V_{pn}(Z,N) = \frac{1}{4}[\{B(Z,N) - B(Z,N-2)\} - \{B(Z-2,N) - B(Z-2,N-2)\}].$$

+	-	-	+
2n 2p	2p	2n	
N-2 Z-2	N-2 Z-2	N-2 Z-2	N-2 Z-2

$$\delta V_{pn}(Z,N) \approx \frac{\partial^2 B}{\partial Z \partial N}.$$

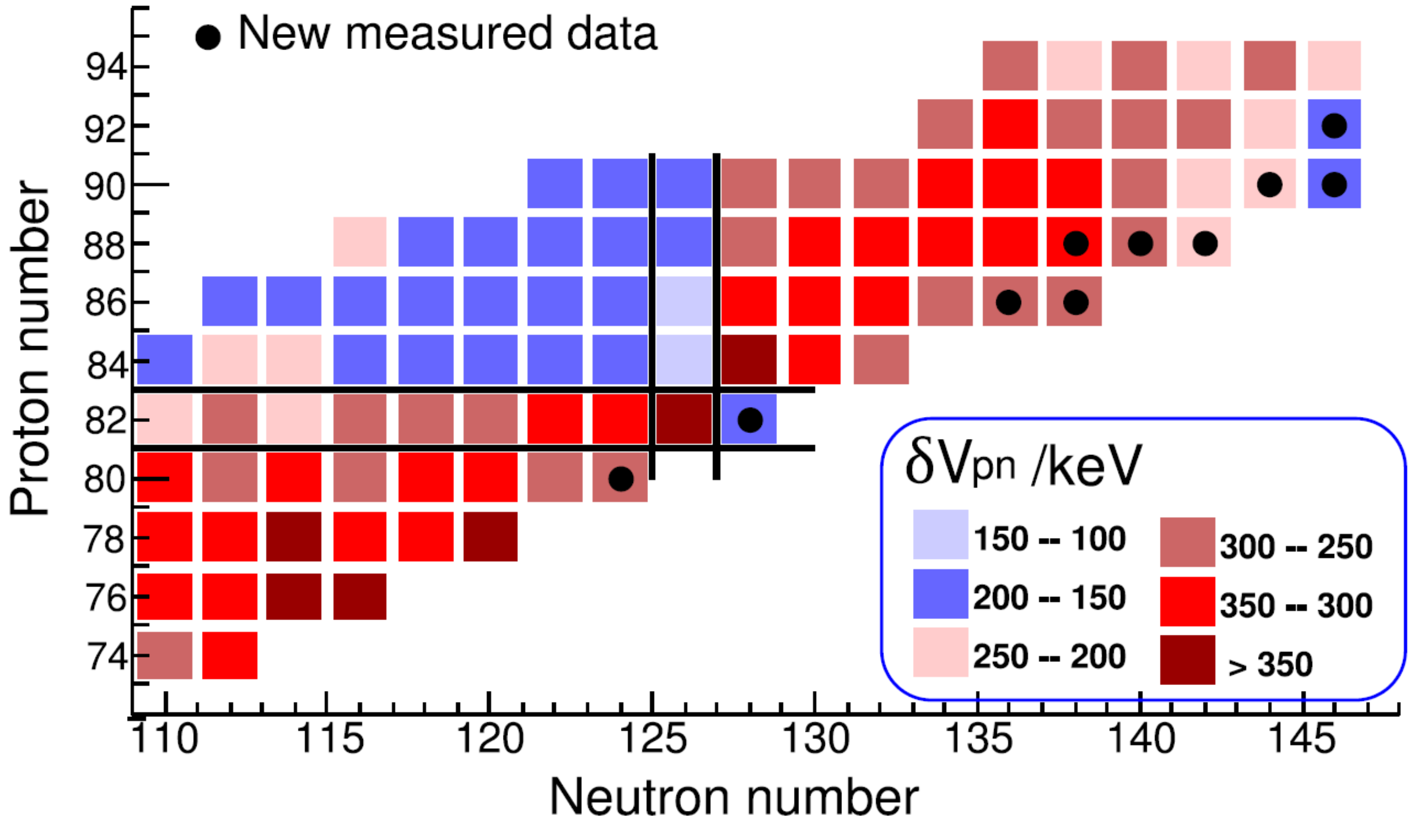

Figure 4.24: Experimental proton-neutron interactions.

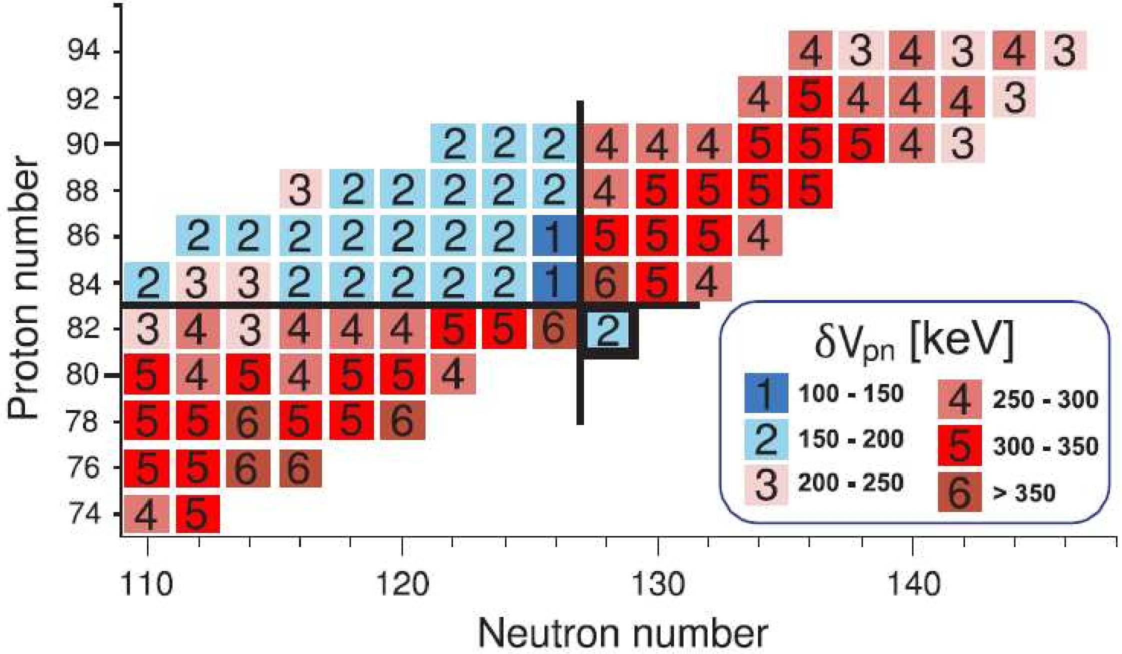

FIG. 3 (color online). Experimentally known δV_{pn} values on the chart of nuclides. Only even-even nuclei are considered. Four quadrants are defined by the $Z = 82$ proton and $N = 126$ neutron shell closures. The diagonal symmetry in the δV_{pn} values for lower-left and upper-right quadrants is clearly seen and can be explained by the "symmetry" in the quantum numbers of the single-particle orbitals occupied by the valence nucleons (see text). The δV_{pn} value for ^{210}Pb (indicated with black square) is the first experimental result in the lower-right quadrant. It has a similar magnitude as the δV_{pn} values in the upper-left quadrant.

Sequence of shell orbitals (R.Casten)

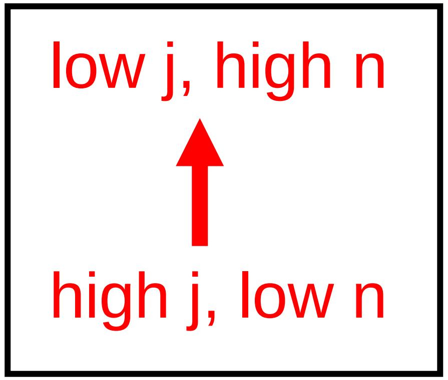

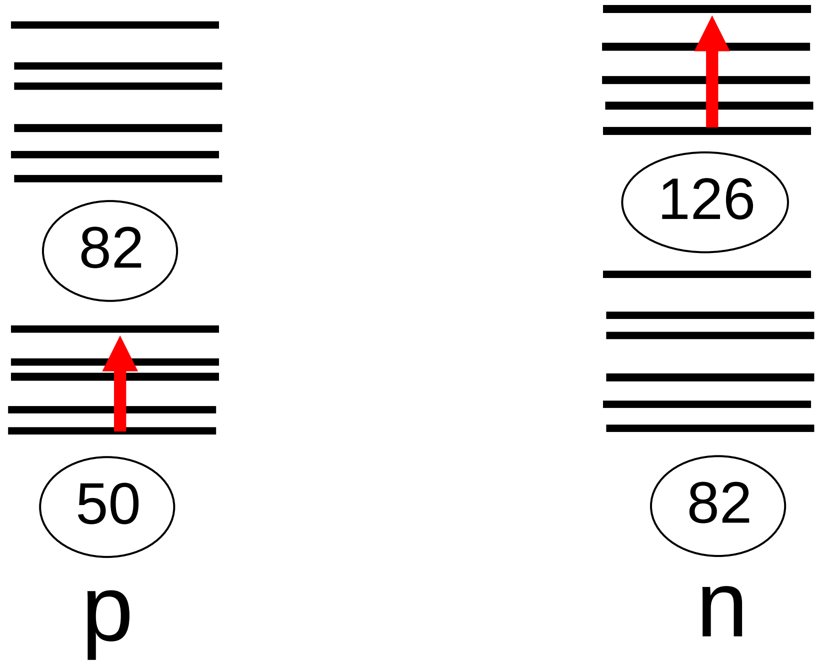

If the protons and neutrons are filling similarly (similar **fractional filling**), the p-n interaction should be largest.

Single-particle levels in the Nilsson spherical potential

N=2(nr-1)+l, liczba węzłów rad. funkcji falowej nr-1

N	nr,l – j	deg.
6	**1i-11/2**	**12**
6	**3d-5/2**	**6**
6	**2g-9/2**	**10**
	=========126	
6	**1i-13/2**	**14**
5	**3p-1/2**	**2**
5	**3p-3/2**	**4**
5	**2f-5/2**	**6**
5	**2f-7/2**	**8**
5	**1h-9/2**	**10**
	========82	
5	**1h-11/2**	**12**
4	**3s-1/2**	**2**
4	**2d-3/2**	**4**
4	**2d-5/2**	**6**

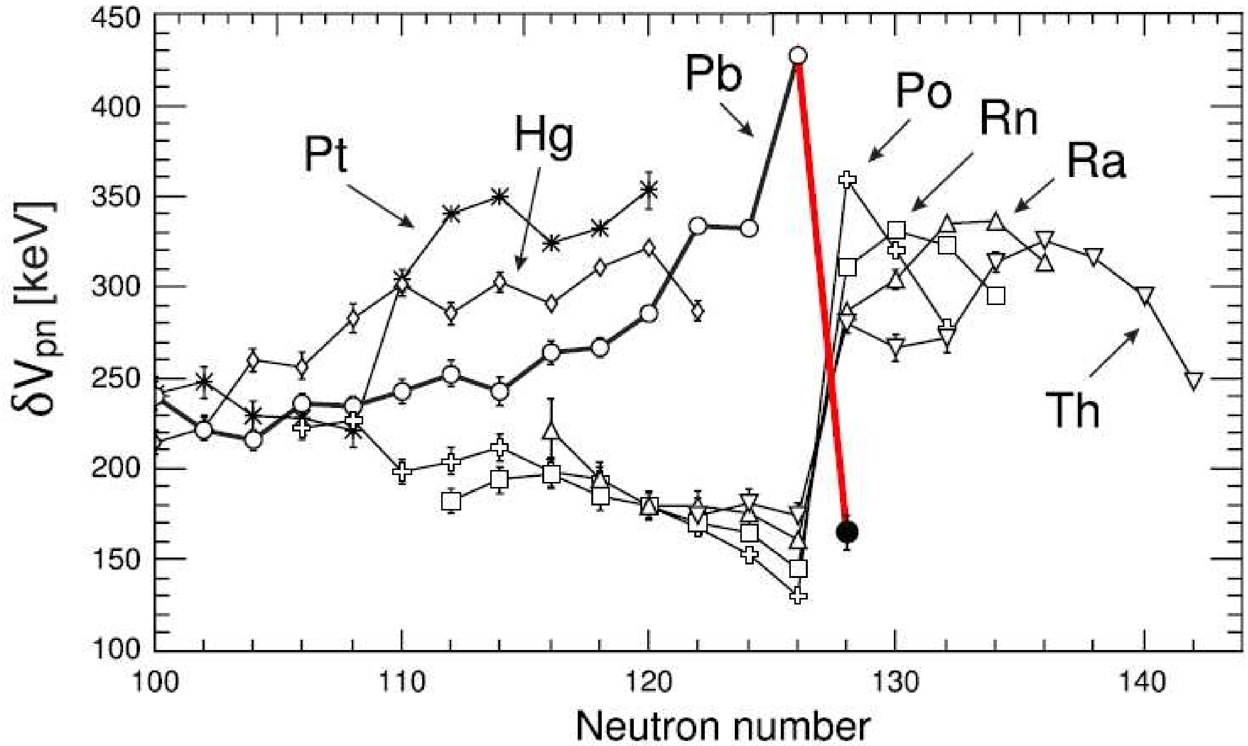

FIG. 2 (color online). Experimentally known δV_{pn} values for isotopic chains below and above the $Z = 82$ proton closed shell. Only even-even nuclei are considered. If not shown the error bars are within the symbol size. The newly obtained δV_{pn} value for ^{210}Pb is emphasized by a filled symbol and the sharp drop from ^{208}Pb to ^{210}Pb is highlighted.

Liquid Drop Model of Nuclear Binding Energy

The binding energy (B) per nucleon is approximately the same for all (stable) nuclei (first noticed in the early 1930s).
This led Weizsa¨cker in 1935 to the comparison of the nucleus with a liquid drop, which also has a constant density, independent of the number of molecules.

$$M_{atom}c^2=N*M_nc^2+Z*M_pc^2-B_N+Z*M_ec^2-B_e$$

B_{LD} (MeV) =			B/A(Pb)
+15.74063	A	volume	15.7
-17.61628	$A^{2/3}$	surface	-3.0
-23.42742	$(N-Z)^2/A$	symmetry	-1.0
- 0.71544	$Z^2/A^{1/3}$	Coulomb	-3.9
-12.59898	$(\mathrm{mod}(N,2)+\mathrm{mod}(Z,2)-1)/A^{1/2}$	pairing	

B/A(Pb)=7.8 MeV

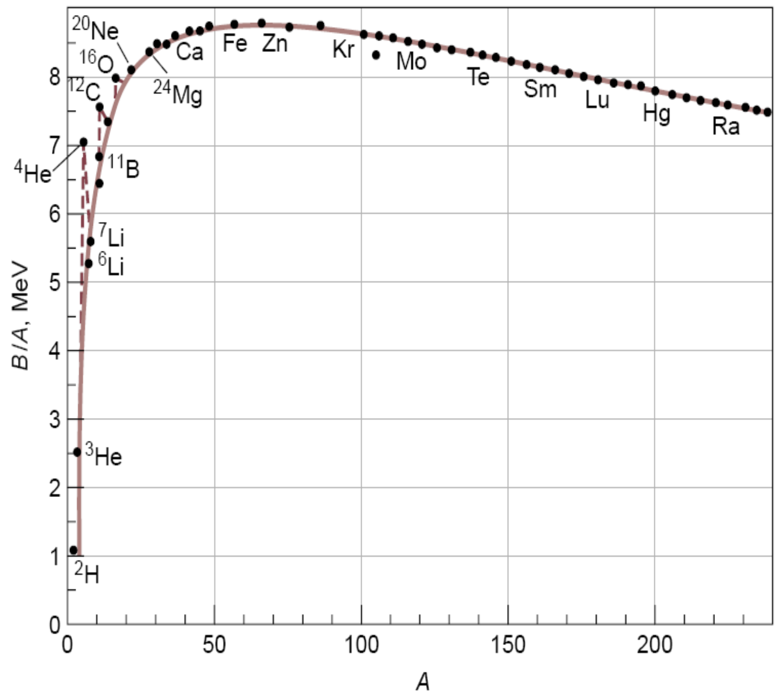

Rms=2.82 MeV

Fitted for 2049 nuclei

$\delta B/A = 3.5*10^{-3} B/A$

(Experimental mass from AME-2003)

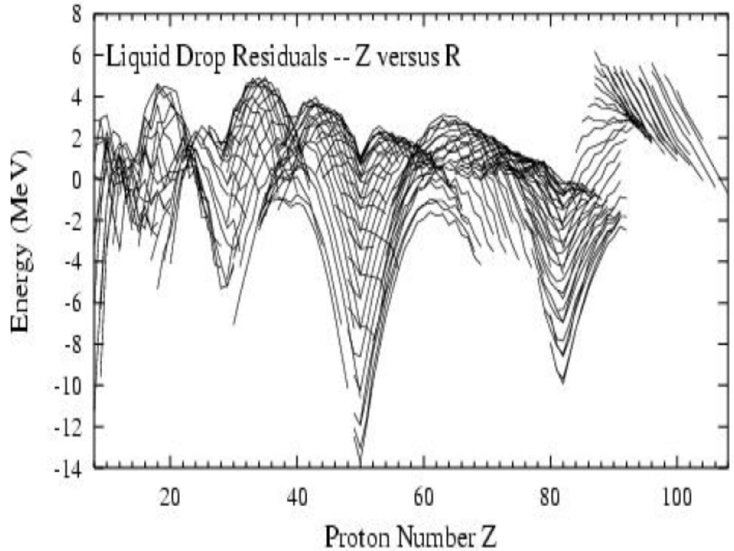

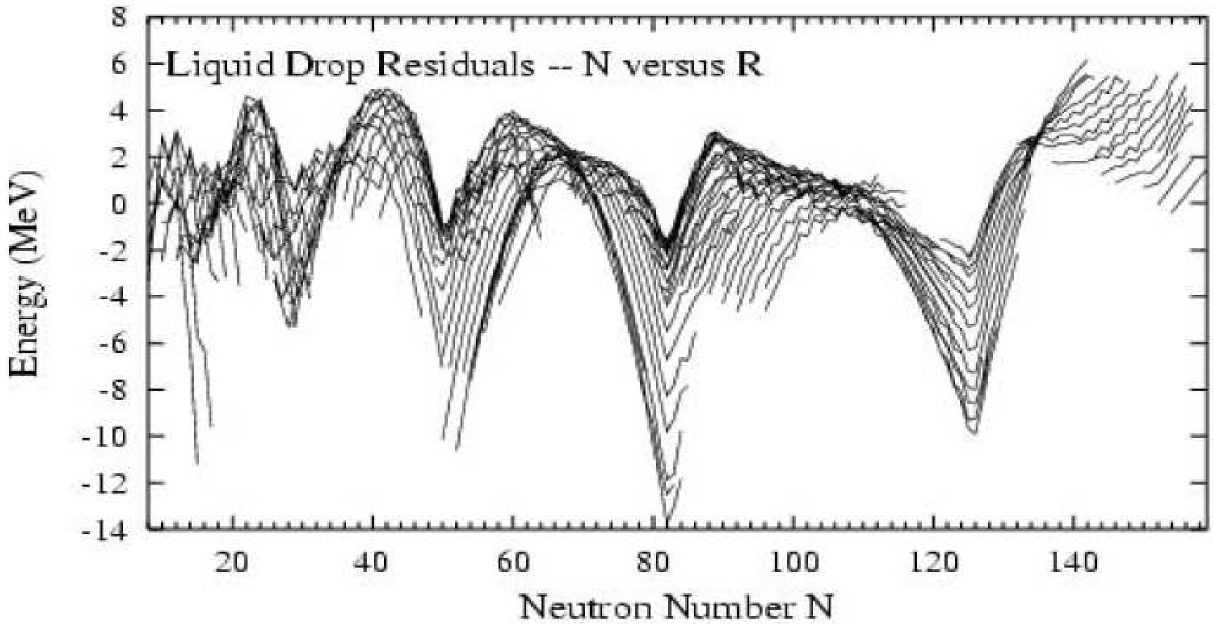

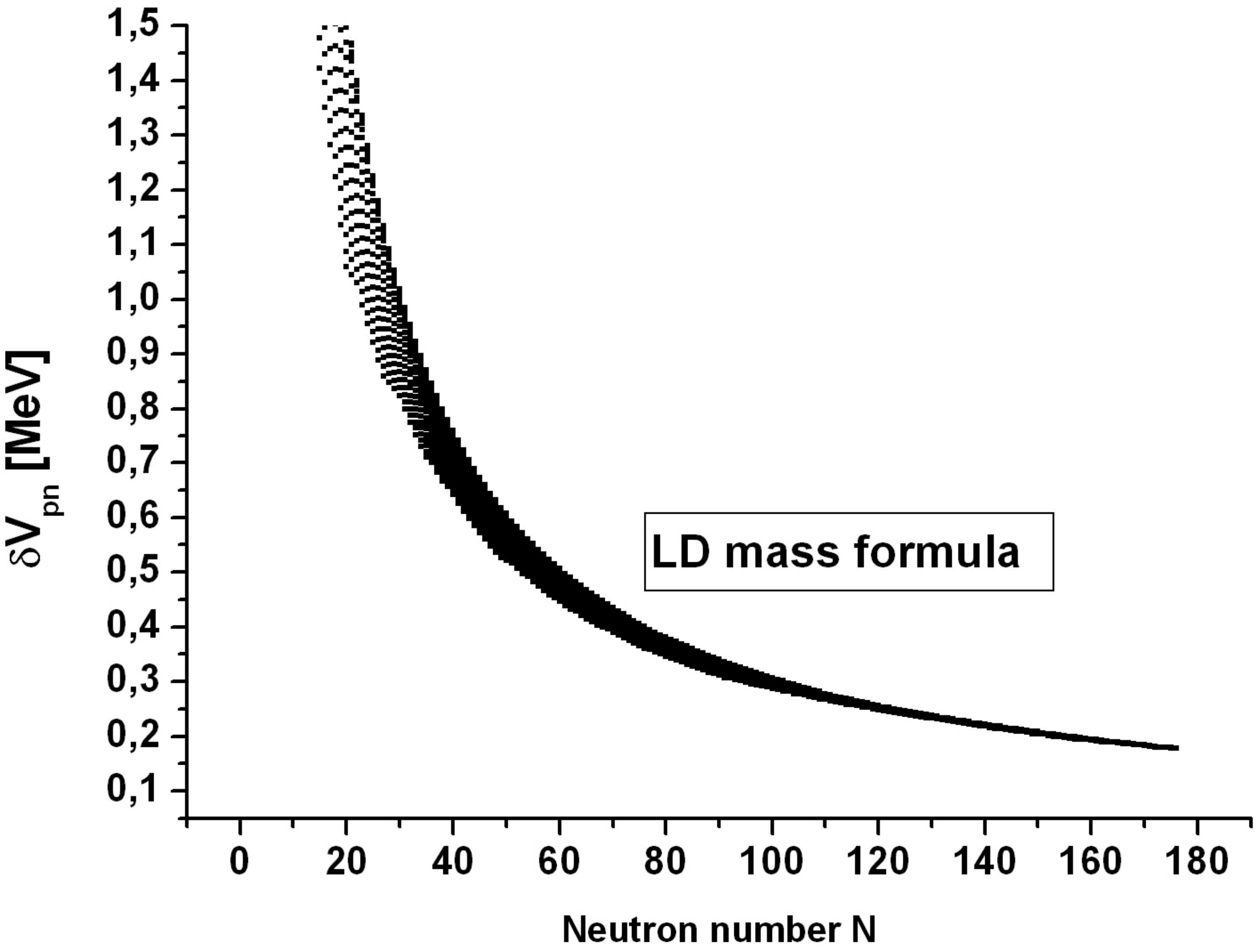

LD mass formula
δVpn [MeV]
1,5
1,4
1,3
1,2
1,1
1,0
0,9
0,8
0,7
0,6
0,5
0,4
0,3
0,2
0,1
0
20
40
60
80
100
120
140
160
180
Neutron number N

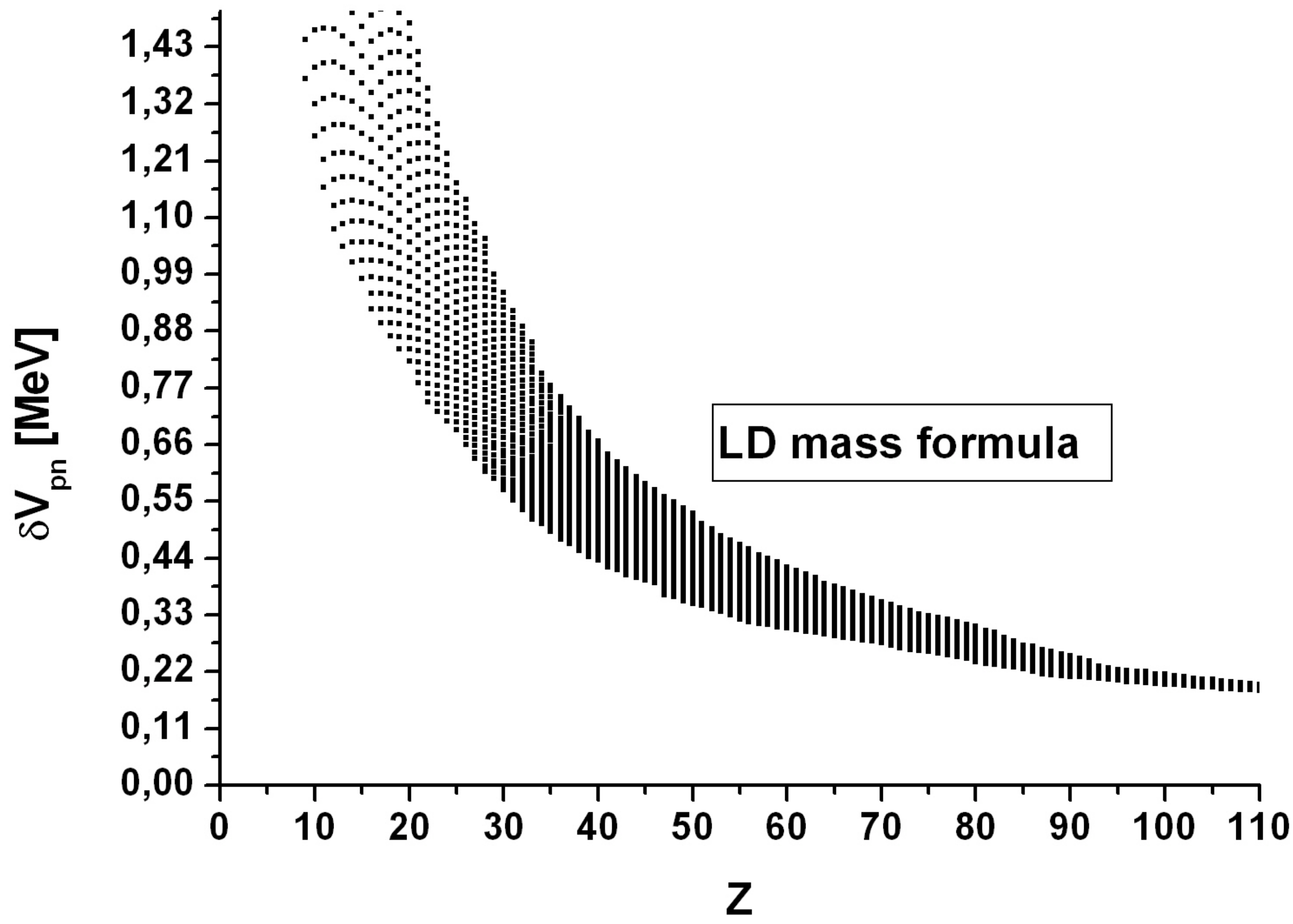

LD mass formula
δV_pn [MeV]
Z
1,43
1,32
1,21
1,10
0,99
0,88
0,77
0,66
0,55
0,44
0,33
0,22
0,11
0,00
0
10
20
30
40
50
60
70
80
90
100
110

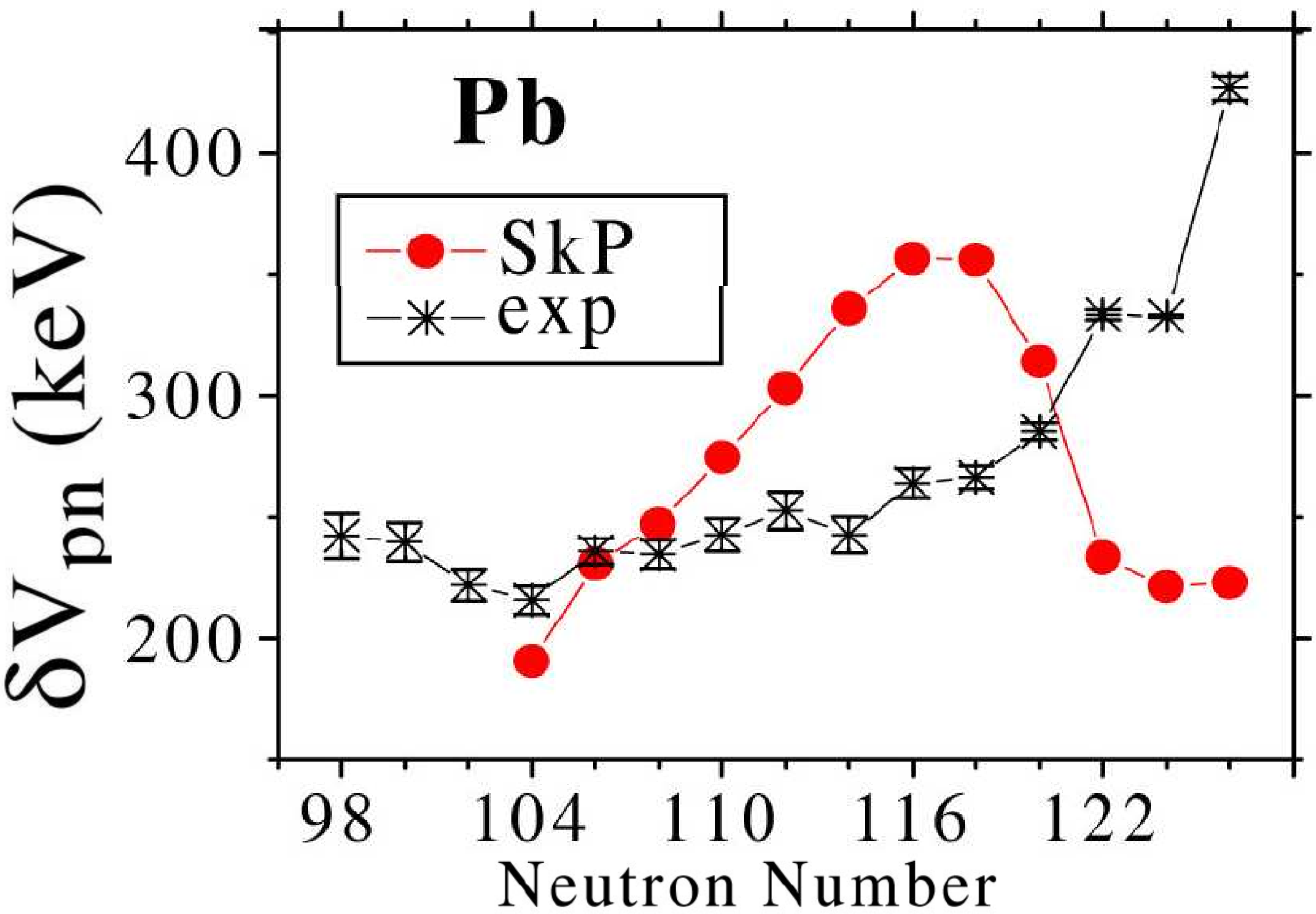

PRL 98, 132502 (2007) PHYSICAL REVIEW LETTERS week ending 30 MARCH 2007

Empirical Proton-Neutron Interactions and Nuclear Density Functional Theory: Global, Regional, and Local Comparisons

M. Stoitsov,[1,2,3] R. B. Cakirli,[4,5] R. F. Casten,[4] W. Nazarewicz,[1,2,6] and W. Satuła[6]

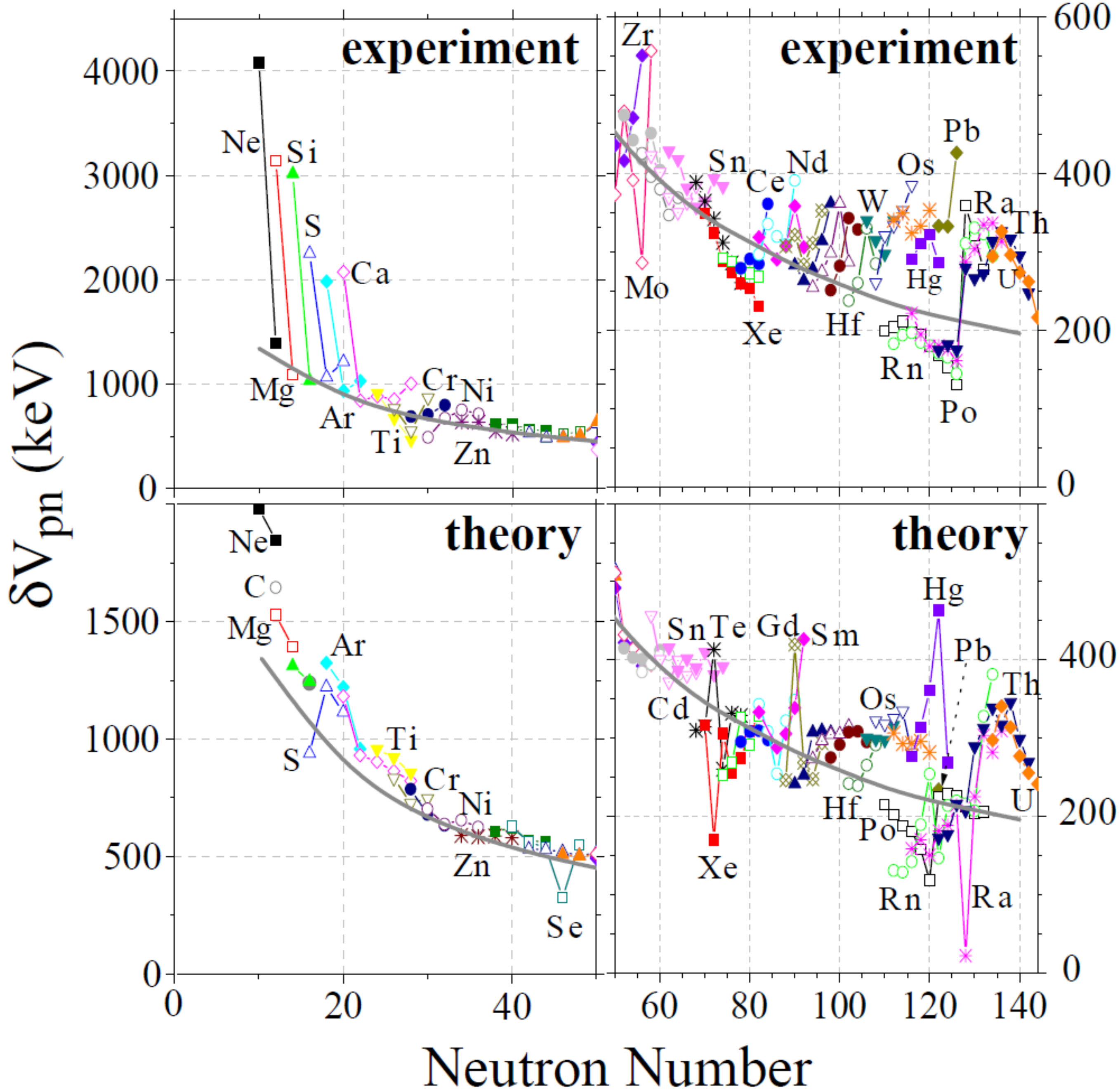

experiment
experiment
theory
theory
δV_pn (keV)
Neutron Number
Ne
Si
S
Ca
Mg
Ar
Ti
Cr
Ni
Zn
Zr
Mo
Sn
Ce
Nd
Xe
W
Os
Pb
Hf
Hg
Ra
Th
U
Rn
Po
C
Se
Te
Gd
Sm
Cd

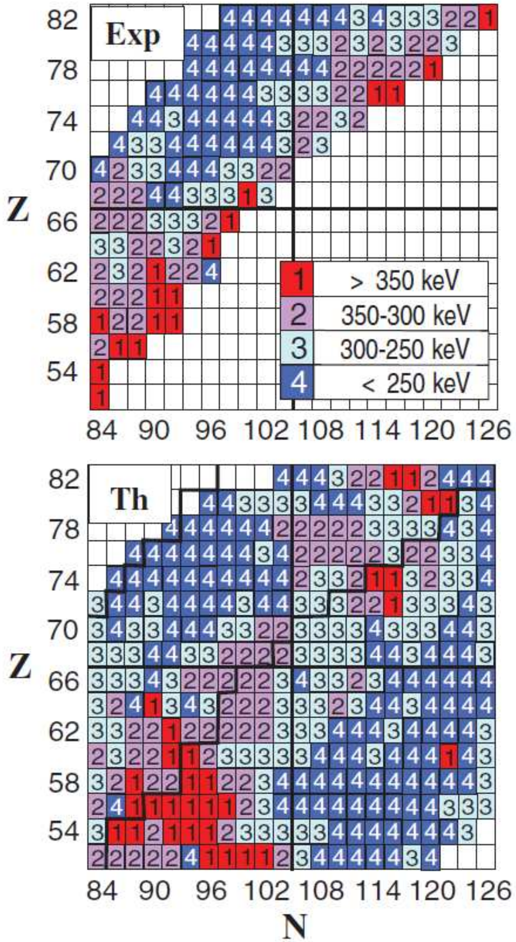

$$\widetilde{\delta V}_{pn} \approx 2(a_{\rm sym} + a_{\rm ssym}A^{-1/3})/A,$$

FIG. 4 (color). Empirical and calculated δV_{pn} values for the major shells $Z = 50$–82, $N = 82$–126, color coded according by magnitude [red for the largest values, blue for the smallest]. (Upper panel taken from Ref. [5]). The zig-zag lines in the theoretical panel enclose nuclei with known empirical δV_{pn} values. Four boxes within these lines are empty since some of the nuclei involved are calculated to lie beyond the proton drip line and cannot be calculated reliably by the current DFT model.

Procesy R(apid) i S(low) syntezy jąder cięższych od żelaza ^{56}Fe, zachodzące w gwiazdach

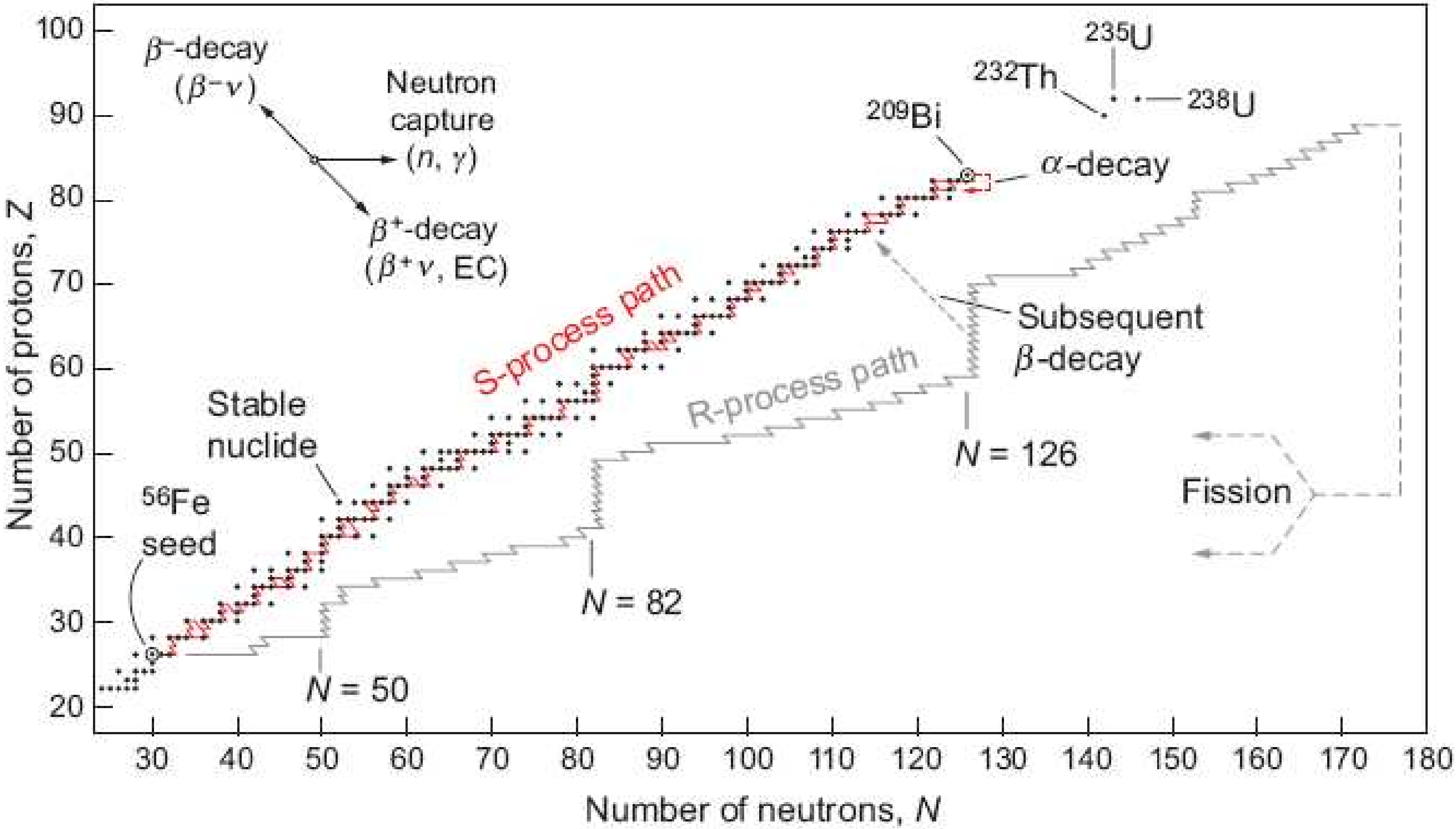

Mass measurements at NuSTAR/FAIR (ILIMA)

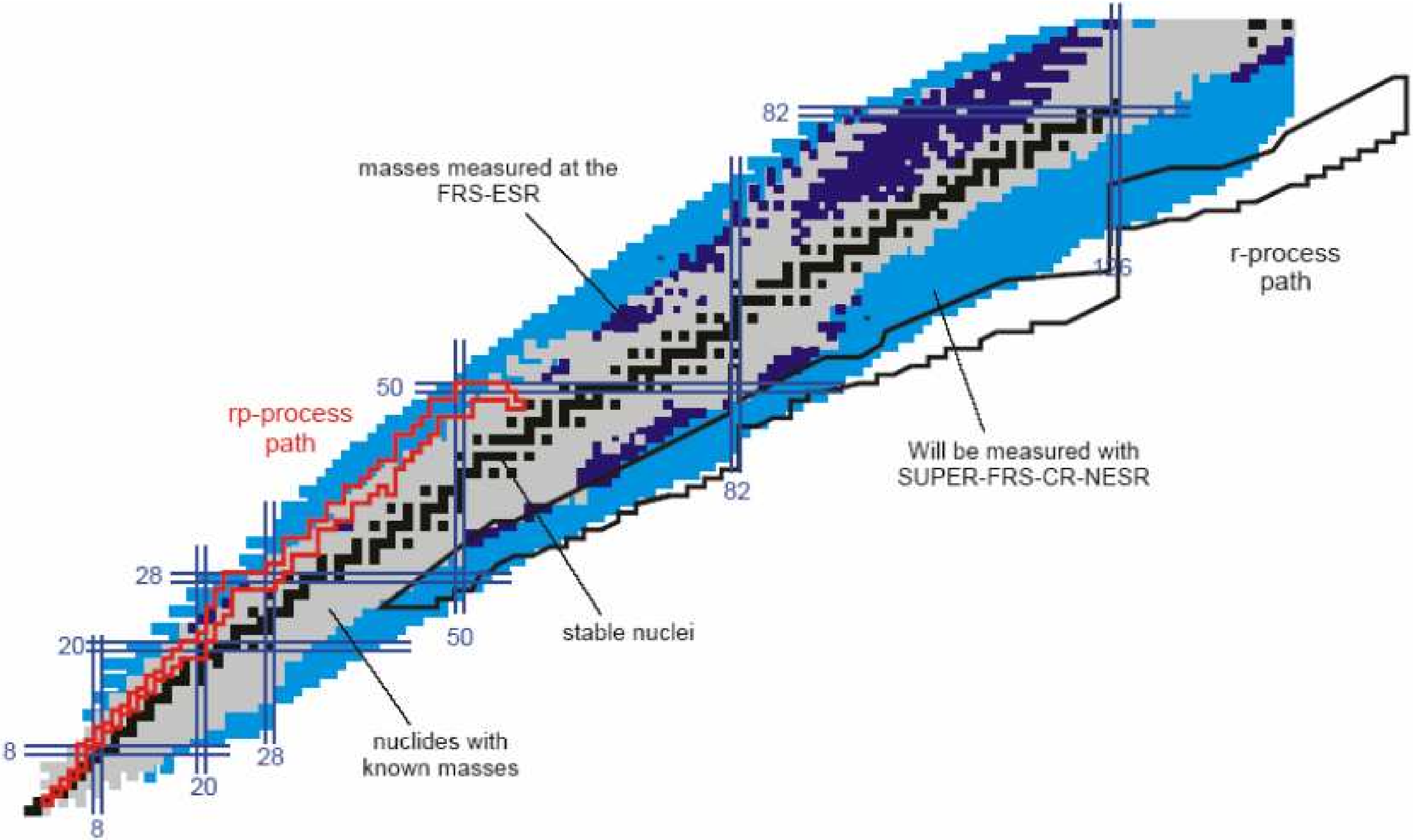

Wnioski

1. **Metodą SMS zmierzono masy dla około 35 jąder atomowych z dokładnością ok. 30 keV.**
2. **Pomiar masy dla jądra 208Hg pozwolił wyznaczyć doświadczalną wartość oddziaływania walencyjnych protonów i neutronów w jądrze 210Pb.**
3. **Interpretacja relacji masowych: szczeliny energetycznej i oddziaływania p-n powinna być skorelowana z innymi obserwablami takimi jak deformacje jąder, energie przejść E2 i E4.**